

## SEARCH FOR $\pi K$ -ATOMS WITH DIRAC-II

Yves Allkofer\*, C. Amsler, S. Horikawa, C. Regenfus, J. Rochet  
*Physik-Institut der Universität Zürich, CH-8057 Zürich, Switzerland*<sup>†</sup>

### Abstract

DIRAC II experiment searches for the electromagnetically bound system  $K^+\pi^-$  (and  $K^-\pi^+$ ) and will measure its lifetime. The latter is related to the S-wave  $K\pi$  - scattering lengths which are of considerable interest to test chiral perturbation predictions involving the  $s$ -quark. There are large uncertainties in the  $K\pi$  - scattering lengths which are obtained by extrapolation to low energies from the poorly known  $K\pi$  isospin 1/2 and 3/2 phase shifts. The  $K\pi$  atoms will be produced with 24 GeV/ $c$  protons from the CERN PS impinging on a target, and their dissociation products analysed by the DIRAC spectrometers. For particle identification the momentum distribution of  $\pi$ ,  $K$  and  $p$  requires aerogel Čerenkov counters with a small index of refraction in the range 1.008 to 1.015. We will report on the status of the experiment.

---

\* talk given by Y. Allkofer. *E-mail address:* Yves.Allkofer@cern.ch

<sup>†</sup> on behalf of the DIRAC collaboration

## 1 The DIRAC experiment and its upgrade

DIRAC is a running experiment at the CERN PS using a 24 GeV/c proton beam on a fixed Ni or Pt-target where *pionium*, a bound state between two opposite charged pions is produced. Up to now 15 000 pairs originating from pionium were detected, which leads to a precision of its lifetime  $\tau$  of 10%. Including systematics and theoretical uncertainties one obtains,

$$\tau = (2.91_{-0.62}^{+0.49}) \cdot 10^{-15} s, \quad (1)$$

see ref. <sup>1)</sup>. In this bound state the strong interaction between the two mesons changes the width (lifetime) of pionium. It can be shown, see ref. <sup>2)</sup> that the lifetime can be expressed as a combination of the S-wave scattering lengths  $a_0^0$  and  $a_2^0$  for isospin 0 and 2 respectively,

$$\frac{1}{\tau} = \frac{2\alpha^3}{9} p^* |a_0^0 - a_2^0|^2 (1 + \delta), \quad (2)$$

where  $p^*$  is the  $\pi^0$ -momentum in the pionium system,  $\alpha$  the fine structure constant and  $\delta = (5.8 \pm 1.2) \cdot 10^{-2}$  accounts for corrections terms.

*Chiral perturbation theory*, (ChPT) describes the hadronic interactions according to the Standard Model at low energies i.e. below the chiral breaking symmetry which is slightly below 1 GeV/c. Very precise predictions are achieved, see ref. <sup>3)</sup>, for the  $\pi\pi$  S-wave scattering length and hence for the pionium lifetime,

$$\tau = (2.9 \pm 0.1) \cdot 10^{-15} s. \quad (3)$$

The agreement between what has been measured by the DIRAC collaboration and the prediction using ChPT is very encouraging. Many efforts have been done to extend the 2-flavor space to the 3-flavor space introducing the  $s$ -quark leading to a SU(3) ChPT. However, in contrast to the SU(2) ChPT the situation is much more confused. Already between different theoretical approaches there is no agreement anymore as shown in fig.1 where the dark shaded ellipse on the left are the results from ref. <sup>4)</sup> based only on ChPT for the  $\pi K$ -scattering lengths and the light shaded ellipse on the right are the results from ref. <sup>5)</sup> using Roy-Steiner dispersion relations.

From the experimental side the last results from scattering experiments were performed in the 70s based on the so called *one pion exchange* (OPE)

model. As an example, in ref. 6) the  $\pi K$  scattering lengths have been measured to be

$$m_\pi \cdot (a_{1/2}^0 - a_{3/2}^0) = 0.475 \pm 0.009, \quad (4)$$

where 1/2 and 3/2 stand for the isospin. This result is far outside the range of fig.1.

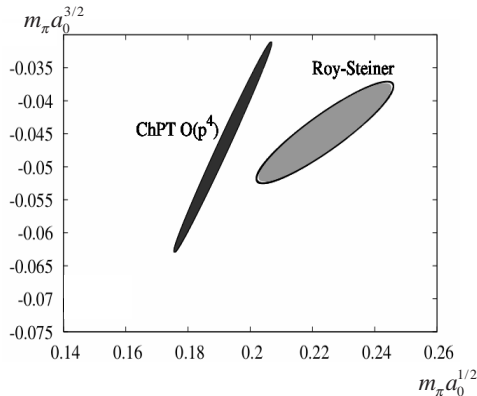


Figure 1: Predicted S-wave  $\pi K$ -scattering length (isospin 1/2 and 3/2) using different theoretical approaches; the  $1\sigma$ -ellipse obtained using ChPT, ref. 4), is shown on the left and the ellipse using the Roy-Steiner dispersion relations, ref. 5), is shown on the right.

In order to clarify this situation it is crucial to perform a new experiment which aims to measure the  $\pi K$ -scattering length with small uncertainties. Similarly to ponium it is possible to relate the lifetime of  $\pi K$ -atoms to the corresponding S-wave scattering lengths,

$$\frac{1}{\tau} = \frac{8\alpha^3}{9} \left( \frac{M_\pi M_K}{M_\pi + M_K} \right)^2 p^* (a_{1/2} - a_{3/2})^2 (1 + \delta), \quad (5)$$

see ref. 7).

## 2 The upgrade to DIRAC II

The DIRAC II experiment aims to measure the lifetime of  $\pi K$ -atoms with a precision of 20%, leading to a determination of the  $\pi K$ -scattering length

difference  $|a_{1/2}^0 - a_{3/2}^0|$  with an accuracy of about 10% which would be the first test of the SU(3)-ChPT predictions in a model independent way. DIRAC II aims to measure simultaneously the lifetime of ponium in order to achieve 6% accuracy on the lifetime, leading to 3% on the scattering length difference  $|a_0 - a_2|$ . To obtain such a precise measurement the DIRAC-spectrometer had to be upgraded to reduce systematic errors and to improve the data collection efficiency. Also crucial for the observation of  $\pi K$ -atoms is the introduction of two new Čerenkov detectors for kaon identifications. The new spectrometer is shown in fig.2.

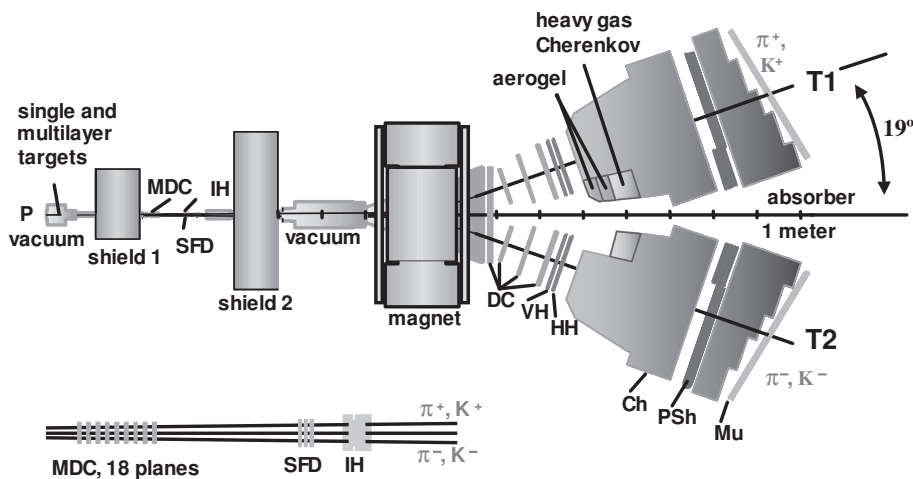


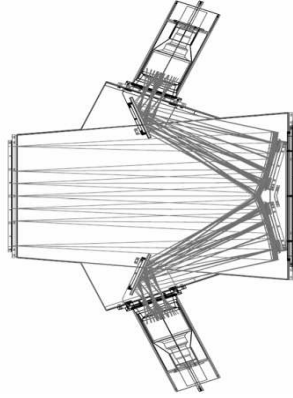
Figure 2: *DIRAC II upgraded spectrometer.* From left to right : micro drift chambers (MDC), scintillating fiber detector (SFD), ionization hodoscope (IH), spectrometer magnet, drift chambers (DC), vertical and horizontal hodoscopes (VH,HH), aerogel Čerenkov detector, heavy gas Čerenkov detector,  $N_2$ -Čerenkov detector, preshower detector (PSh) and muon detector (Mu).

## 2.1 Upgrade of the existing setup

A new tracker, the micro drift chambers (MDC) has been installed to improve track reconstruction upstream of the target. To detect atomic pairs immediately behind the magnet one has to distinguish two tracks with a very small opening angle. This task is fulfilled by this detector with a spatial resolution



(a)



(b)

Figure 3: a) Photograph of the heavy gas Čerenkov detector installed in the negative spectrometer arm; b) Sketch of the inner part of the heavy gas detector showing the Čerenkov light propagation. The photons are first reflected backwards on a set of four spherical mirrors and then focused on the photocathod by flat mirrors.

which is estimated to be around  $22 \mu\text{m}$  for single tracks and less than  $200 \mu\text{m}$  for double tracks, with a detection efficiency higher than 98%.

The scintillating-fiber detector (SFD) has also been upgraded. In the new detector fibers  $0.27 \text{ mm}$  in diameter are used instead of  $0.5 \text{ mm}$  in the previous version to improve the double-track resolution. Also, new readout electronics equipped with both ADC and TDC has been developed. The new TDC has  $120 \text{ ps}$  time resolution which is four times better than the old one.

New shielding has been installed, see fig.2 (shield 1 and 2), to reduce the number of accidentals. This allows to run with much higher primary beam intensity without increasing the deadtime of the detectors.

The vertical and horizontal hodoscopes (VH,HH) are located after the Drift Chambers (DC) which are DIRAC's main trackers. They have been enlarged to increase the aperture of the DIRAC spectrometer by 10% in the region where kaons from ionized  $\pi K$ -atoms are expected. Also at the very end of the spectrometer the muon detectors (Mu) have been enlarged for the same

reason.

Electrons are rejected using two detectors, the  $N_2$ -Čerenkov detector (Ch) and the preshower detector (PSh). The Ch-detector had to be cut in the central part to make room for the new aerogel and heavy gas Čerenkov detectors. This limits significantly the electron-rejection efficiency in this area. These losses have been compensated by a second layer of the PSh detector in the critical region and by reducing the sizes of the scintillator slabs by a factor of two. All

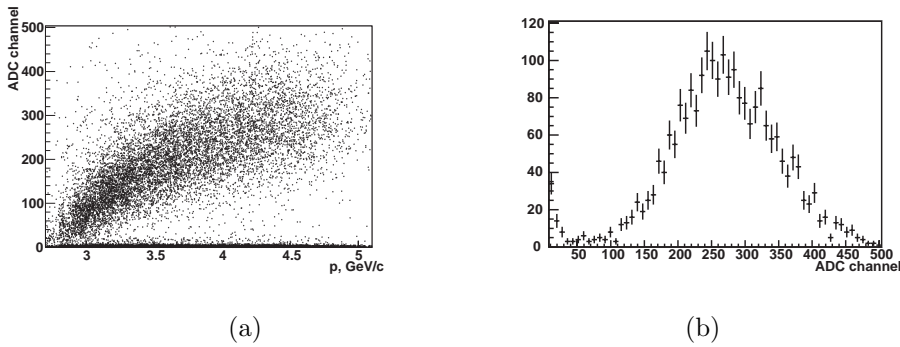


Figure 4: a) *ADC channels vs. momentum for one of the four photomultipliers of the heavy gas Čerenkov detector*; b) *integrated pulse height spectrum for a pion momentum of  $p_\pi = 4 \text{ GeV}/c$ .*

these modifications led to a detection efficiency increasing by a factor of more than two and to a strong reduction of systematic errors.

## 2.2 Kaon identification

Since kaon identification is crucial for the measurement of  $\pi K$ -atoms the two new Čerenkov detectors used for this purpose will be discussed more in detail in this section.

### 2.2.1 Heavy gas Čerenkov detector

The heavy gas Čerenkov detector shown in fig.3 detects pions and can be used in coincidence for the  $\pi\pi$ -atoms measurement to reduce systematics compared to earlier data (2001-2003), or in anti-coincidence for  $\pi K$ -atoms observation.

The  $C_4F_{10}$  gas used as radiator is cleaned continuously through a recirculation system, see ref. 8), to achieve high purity. Each module is read out by four 5" photomultipliers (PM). Their response is shown in fig.4a) as a function of pion-momentum. The associated pulse height spectrum is shown in fig.4b). Once calibrated the sum of all PMs leads to 20-25 photoelectrons and hence to a pion detection/rejection efficiency higher than 99.5% for  $p_\pi \geq 4\text{GeV}/c$ .

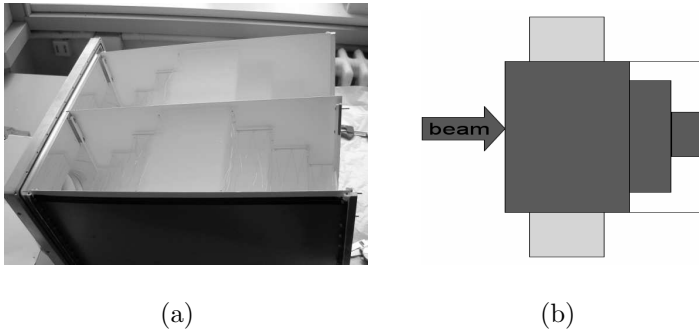


Figure 5: a) Photograph taken during the assembly of the two heavy aerogel modules illustrating the steps of the pyramid design; b) Side view of the pyramid design with the two PMs on the top and the bottom.

### 2.2.2 Aerogel Čerenkov detector

The aerogel Čerenkov detector consists of three independent modules read out by two 5" PMs each. Because of the large momentum range to cover two refractive indices are used:  $n = 1.015$  and  $n = 1.008$ . DIRAC requires to cover a large area, especially vertically. This implies the need for a more tricky design than is usual for ordinary threshold counters. In fact, the large distance between the two PMs of one module decreases strongly the number of collected photons and leads to a strong dependence on the impact position of the incoming particle: due to the strong absorption in aerogel, a track crossing close to one PM will give a better light collection efficiency than one crossing near the center of the counter. To compensate for this absorption the thickness of the radiator in the middle of the detector has been increased. This is the so-called *pyramid design*, see fig.5. To compensate for the small number of

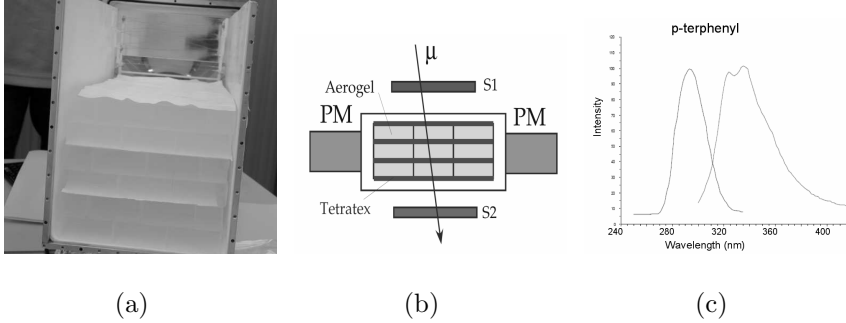


Figure 6: a) Photograph taken during the assembly of the light aerogel module illustrating the wavelength shifter (WLS) coated Tetratex layers; b) Side view of the sandwich design alternating aerogel and WLS coated Tetratex; c) Absorption (on the left) and emission (on the right) spectrum of p-Terphenyl which was chosen as WLS.

Čerenkov light in the  $n = 1.008$  aerogel we developed a *sandwich* detector. It consists of alternating Tetratex (a diffusive reflector) layers coated with a wavelength shifter (WLS) and aerogel layers. Shifting UV-light to blue light reduces the absorption in aerogel which is strongly wavelength dependent, and also improves the detection efficiency of the PMs. The design is shown in fig.6 as well as the absorption and emission spectrum of p-terphenyl, the WLS we finally used. The final detector is shown in fig.7. The integrated pulse height spectrum for kaons is shown in fig.8 using the heavy gas detector in anticoincidence. For the  $n = 1.008$  module kaons are selected to have momenta higher than 5.2 GeV/c and for the  $n = 1.015$  kaons are selected to have a momentum range between 3.75 and 5.2 GeV/c. For a proton rejection factor of typically 40 the kaon detection efficiency averaged over the full operating momentum range is estimated to lie above 85% for the  $n = 1.008$  aerogel, and above 95% for the  $n = 1.015$  one.



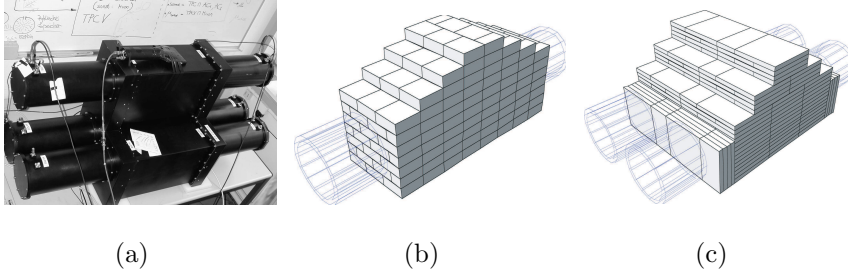


Figure 7: Photograph of the final detector a) including the three modules during laboratory tests with cosmic rays. On the top a scintillating counter is used for triggering. The structure of the aerogel for the  $n = 1.008$  and the two  $n = 1.015$  modules is shown in b), respectively c).

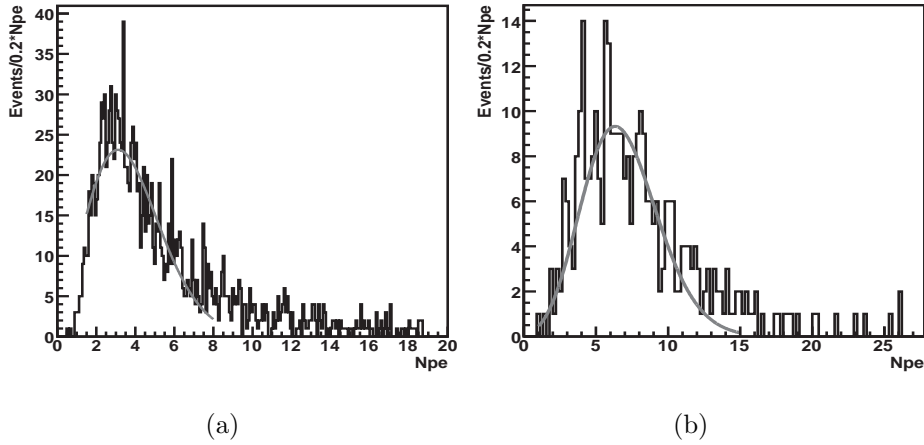


Figure 8: a) Integrated pulse height spectrum showing the kaon signals for momenta above  $5.2 \text{ GeV}/c$  in the  $n = 1.008$  module. b) Same spectrum for selected kaons with momenta between  $3.75$  and  $5.2 \text{ GeV}/c$  in the  $n = 1.015$  module. For both the heavy gas detector is used in anti-coincidence for pion rejection.

### 3 Outlook

The number of  $\pi^-K^+$ - and  $K^-\pi^+$ -atoms detected in 2007 run has been estimated as follows. The ratio between the number of ionized  $\pi\pi$ - and  $\pi K$ -atoms (including  $\pi^-K^+$ - and  $K^-\pi^+$ -atoms) was simulated to be 15 using FRITIOF 7.02, see ref. <sup>9</sup>). In 2001 we obtained 1600  $\pi\pi$ -atoms per month. For 2007 this number has to be multiplied by a factor of two for the improved detection efficiency due to the spectrometer upgrade. This leads to 190  $\pi K$ -atoms detected per month. The last correction comes from the different ionization probabilities for Ni (31%) and Pt-target (55%) used in 2001 and in 2007. We expect to detect about 1400  $\pi K$ -atomic pairs during 4 months of data taking, which would lead to the observation of  $\pi^-K^+$ - and  $K^-\pi^+$ -atoms with a significance of more than  $3\sigma$ , taken the expected background into account.

### References

1. B. Adeva *et al.* (DIRAC collaboration), Phys. Lett. **B619**, 50 (2005)
2. J. Gasser *et al.*, Phys. Rev. **D64**, 016008 (2001)
3. G. Colangelo *et al.*, Nucl. Phys. **B603**, 125 (2001)
4. V. Bernard *et al.*, Nucl. Phys. **B357**, 129 (1991)
5. P. Buettiker *et al.*, Eur. Phys. J **C33**, 409 (2004)
6. P. Estabrooks *et al.*, Nucl. Phys. **B133**, 490 (1978)
7. J. Schweizer, Phys. Lett. **B587**, ) 33 (2004)
8. Y. Allkofer *et al.*, Proc. 6th Int. Workshop on Ring Imaging Cherenkov Counters (RICH2007), Trieste, in print (2007)
9. B. Nilsson-Almqvist, E. Stenlund, Com. Phys. Comm. **43**, 387 (1987).